

## TeV $\gamma$ -Ray Observations of the Perseus Galaxy Cluster

J.S. Perkins<sup>a</sup> and the VERITAS Collaboration<sup>b</sup>

(a) Washington University in St. Louis, St. Louis, MO 63130 USA

(b) For full author list, see J. Holder's paper "Status and Performance of the First VERITAS Telescope" from these proceedings

Presenter: J.S. Perkins (jperkins@physics.wustl.edu), usa-perkins-JS-abs1-og23-oral

We report on observations of the Perseus cluster of galaxies using the 10 m Whipple  $\gamma$ -ray telescope during the 2004-2005 observing season. We apply a two dimensional analysis technique to allow us to scrutinize the cluster for TeV emission. In this contribution we will first calculate flux upper limits on TeV  $\gamma$ -ray sources within the cluster. Second, we derive an upper limit on the extended cluster emission. We then compare the flux upper limits with the EGRET upper limit at 100 MeV and theoretical models.

### 1. Introduction

We selected the Perseus cluster based on its closeness ( $z = 0.0179$ , 75 Mpc) and high mass ( $4 \times 10^{14} M_{\odot}$  [5]). In galaxy clusters,  $\gamma$ -rays can originate from cosmic ray electrons (CRe) as Inverse Compton and Bremsstrahlung emission and from the decay of neutral pions produced when cosmic ray protons (CRp) interact with thermal target material. Detection of  $\gamma$ -ray emission from galaxy clusters would make it possible to measure the energy density of these supra-thermal particles in the inter-cluster medium. By combining MeV observations with TeV  $\gamma$ -ray observations we may be able to disentangle the various components that contribute to the emission [20, 14]. In addition to a cosmic ray (CR) origin of  $\gamma$ -rays, annihilating dark matter may also emit  $\gamma$ -rays. The intensity of the radiation depends on the nature of dark matter, the annihilation cross sections, and the dark matter density profile close to the core of the cluster [8].

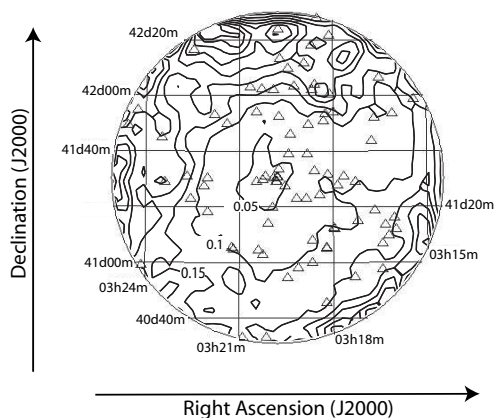


**Figure 1.** 90% upper limit map from point sources of the inner 1 degree of the Perseus cluster of galaxies. The scale is in units of the flux from Crab Nebula with each contour step equal to 0.05 times the Crab flux. Select contours are labeled. The triangles are radio sources, some of which can be found in Table 1.

**Table 1.**  $\gamma$ -ray flux 90% upper limits on the 5 most luminous radio galaxies in the Green Bank 6 cm Radio Source Catalog [6] within the Perseus cluster of galaxies.

Source	RA (J2000)	DEC (J2000)	6 cm Flux (mJy)	TeV Flux Upper Limit (Crab)   (ergs cm <sup>-2</sup> s <sup>-1</sup> )	
GB6 J0319+4130	03 19 47.1	+41 30 42	46894	0.047	$0.37 \times 10^{-11}$
GB6 J0318+4153	03 18 16.0	+41 53 14	15124	0.10	$0.78 \times 10^{-11}$
GB6 J0316+4118	03 16 40.9	+41 18 49	264	0.14	$1.1 \times 10^{-11}$
GB6 J0317+4054	03 17 19.4	+40 54 40	53	0.19	$1.5 \times 10^{-11}$
GB6 J0319+4223	03 19 44.4	+42 23 24	49	0.34	$2.6 \times 10^{-11}$

## 2. Analysis and Results

We observed the Perseus cluster of galaxies with the Whipple 10 m telescope between August 16, 2004 and February 05, 2005 (UT). Details about the Whipple telescope including the GRANITE-III camera have been given in [4]. Data from the Whipple 10 m are taken as pairs of 28 minute runs. An ON run pointed at the source is followed by an OFF run offset  $7.50^\circ$  in RA for background subtraction. Removing runs with low rates and mismatched ON/OFF pairs results in a usable data set of 29 ON/OFF pairs which corresponds to 810.4 minutes of ON and OFF data. More detailed descriptions of Whipple observing modes and analysis procedures can be found in [21, 15, 13]. The  $\gamma$ -ray selection criteria used in this analysis (EZCuts2004, see [10]) were designed to be independent of zenith angle and energy and are well suited for two-dimensional source localization. The 2D arrival direction of each  $\gamma$ -ray event was calculated from the orientation and elongation of the light distribution [2]. We estimate a mean energy threshold for the Whipple 10 m data to be approximately 400 GeV [12]. If not stated otherwise, reported uncertainties are one standard deviation and upper limits are given at the 90% confidence level. The results given here are preliminary. Further analysis of systematic error is in progress.

In order to search for point sources within the field of view, the camera resolution and efficiency need to be known to good accuracy at all points. We used an empirical method based upon data from the Crab Nebula that was taken during the same months as Perseus. For the Crab Nebula, we used 24 ON/OFF pairs with the camera centered on the Crab, two pairs at an offset of 0.5 degrees and three pairs at an offset of 0.8 degrees resulting in a total on time of 670.7, 55.92 and 83.83 minutes respectively. The Crab data were binned by the square of the distance of the reconstructed shower direction from the location of the Crab Nebula (so as to eliminate any area scaling) and the excess (ON minus OFF) was plotted and fitted with an exponential. This fit gives us a direct measurement of the resolution of the camera from a point source at the three different offsets. From these same data we determined an optimal angular cut based on the integral of the excess as a function of the radius. We also determined how the efficiency of the camera falls off towards the edges by calculating the  $\gamma$ -ray rate at the different offsets.

Using these results we then searched over the entire field of view of the camera for point sources within the Perseus cluster. At every point on the camera, we used the optimal cut specified above and calculated the  $\gamma$ -ray excess from the data. From this excess, we determined the flux in units of Crab. We then used this flux and its error to calculate a Bayes upper limit on the flux [7], taking into account the statistical error on the Crab event rate. See Figure 1 for the upper limit map. Table 1 shows the  $\gamma$ -ray flux upper limit for some of the most luminous radio galaxies within the Perseus cluster from the Green Bank 6 cm catalog [6].

To search for extended emission from the Perseus cluster we assume that the TeV  $\gamma$ -ray surface brightness mimics that of the thermal X-ray emission (as seen from Chandra [17] and BeppoSAX [11]) which arises from

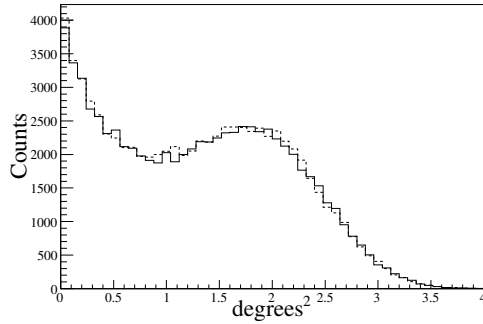


**Figure 2.** Number of Whipple 10 m events versus the average distance of the estimated arrival direction from the center of the field of view squared. The dashed data are the OFF counts and the solid are the ON counts. There is good correlation between the ON and the OFF data out to the edge of the camera, and no excess from the cluster can be recognized.

interactions of the CRs with the thermal photons in the cluster. The X-ray surface brightness can be modeled [14] as a double- $\beta$  profile given by

$$\Sigma(r) = \left( \sum_{i=1}^2 \Sigma_i^2 \left( 1 + \frac{r^2}{r_i^2} \right)^{-3\beta_i/2} \right)^2 \quad (1)$$

where  $\Sigma$  is the surface brightness,  $\Sigma_i$ ,  $r_i$  and  $\beta_i$  are model parameters found in [14] and based on data from [3] and [18].

The emission will continue out to the accretion shock which is expected to occur at  $\sim 2.2^\circ$  from the cluster center. Assuming the double- $\beta$  profile, we estimate that 84% of the total cluster emission comes from within  $0.8^\circ$  from the cluster center. Figure 2 shows the ON and OFF data after analysis and cleaning plotted versus the distance from the center of the field of view squared. There is no obvious excess in Figure 2 out to the edge of the field of view.

We derive a quantitative upper limit by normalizing this profile, smoothed with the Whipple angular resolution, to 1 over the field of view of the camera. We then smoothed the expected emission by the resolution of the Whipple telescope and then multiplied the result by the efficiency curve found from the Crab data to produce an expected rate map. The rate map and actual excess were integrated over the inner  $0.8$  degrees and these two values were used to determine the upper limit on the TeV flux from the entire Perseus cluster. The upper limit on the emission is 0.23 of the Crab flux ( $1.31 \times 10^{-11}$  ergs  $\text{cm}^{-2}$   $\text{s}^{-1}$ ).

### 3. Interpretation and Discussion

Figure 3 shows the upper limit on TeV emission from the cluster and compares it to a previous upper limit from EGRET [16] and with the results of two model calculations. The solid line is a model of CRp induced  $\gamma$ -ray emission normalized to the EGRET upper limit [14]. The  $\gamma$ -ray emission arises from the decay of neutral pions produced when CRp interact with thermal target material. The model assumes that the CRp energy density is 14% of the thermal energy density. The dotted line shows the expected emission derived under the assumption that the TeV emission from the galactic center [1, 9, 19, 8] originates from dark matter annihilation and that the dark matter flux scales with total mass and the inverse of the distance squared. The expected flux is well below the sensitivity of present instruments. Comparison of the upper limits with models of leptonic emission (Bremsstrahlung, Inverse Compton) are in preparation.

Though we did not detect significant TeV  $\gamma$ -rays from the Perseus cluster of galaxies in 841 minutes of observations, we are able to determine two different types of upper limits on the emission: we placed upper limits

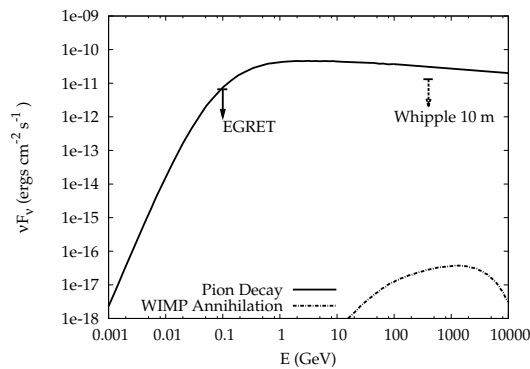


**Figure 3.** The Whipple 90% upper limit on the emission from the Perseus cluster is plotted as a dashed arrow at 400 GeV. The EGRET upper limit from [16] is shown at 100 MeV. The upper limits of the pion decay  $\gamma$ -ray flux from [14] is plotted as a solid line. Also plotted is the dark matter emission derived under the assumption that the TeV  $\gamma$ -ray signal from the galactic center originates from the annihilation of an 18 TeV neutralino [8].

on the emission from point sources within the cluster and we provide an overall upper limit assuming extended emission. The  $\gamma$ -ray data constrain the ratio of energy of the thermal and non-thermal plasmas.

#### 4. Acknowledgments

This research is supported by grants from the U.S. Department of Energy, the National Science Foundation, the Smithsonian Institution, by NSERC in Canada, by Science Foundation Ireland and by PPARC in the UK. J.S. Perkins would like to thank the AAS, the ICRC and the Washington Univ. Physics Dept for travel support.

#### References

- [1] F. A. Aharonian et al., astro-ph/0408145.
- [2] J. H. Buckley et al. *A&A* 329, 639-658 (1998).
- [3] E. Churazov et al., *ApJ* 590, 225 (2003).
- [4] J. P. Finley et al., Proc. ICRC 2001, 2827 (2001).
- [5] M. Giradi et al., *ApJ* 505, 74-95 (1998).
- [6] P. C. Gregory et al., *ApJ Sup.* 103, 427-432 (1996).
- [7] O. Helene, *Nucl. Instrum. Methods* 212, 319 (1983).
- [8] D. Horns, *Phys. Lett. B* 607, 225-232 (2005).
- [9] K. Kosack et al., *ApJ* 608, L97 (2004).
- [10] K. Kosack, "Very High Energy Gamma Rays from the Galactic Center", PhD Thesis, Washington University in St. Louis, 63 (2005).
- [11] J. Nevalainen et al., *ApJ* 608, 166 (2004).
- [12] P. F. Rebillot et al., *ApJ* in preparation (2005).
- [13] P. T. Reynolds et al., *ApJ* 404, 206 (1993).
- [14] C. Pfrommer and T. A. Enßlin, *A&A* 413, 17-36 (2004).
- [15] M. Punch & D. J. Fegan, *AIP Conf. Proc.* 220: High Energy Gamma Ray Astronomy 220, 321 (1991).
- [16] O. Reimer et al., *ApJ* 588, 155-164 (2003).
- [17] J. S. Sanders et al., *MNRAS* 360, 133 (2005).
- [18] M. F. Struble & H. J. Rood, *ApJ Sup.* 125, 35 (1999).
- [19] K. Tsuchiya et al., *ApJ* 606, L115 (2004).
- [20] H. J. Völk, *Aph* 11, 73-82 (1999).
- [21] T. C. Weekes, *Space Sci. Rev.* 75, 1 (1996).